CASANOVA-CARVAJAL, O., URBANO-BOJORGE, A.L., RAMOS, M., SERRANO-OLMEDO, J.J. y MARTÍNEZ-MURILLO, R., 2019. Slowdown intracranial glioma progression by optical hyperthermia therapy: study on a CT-2A mouse astrocytoma model. Nanotechnology, vol. 30, no. 35, ISSN 0957-4484. DOI 10.1088/1361-6528/ab2164.

FULL PAPER

Title page

SLOWDOWN INTRACRANIAL GLIOMA PROGRESSION BY OPTICAL HYPERTHERMIA THERAPY: STUDY ON A CT-2A MOUSE ASTROCYTOMA MODEL

Oscar Casanova-Carvajal[1,2,a], Ana Lorena Urbano-Bojorge[1,2,b] , Milagros Ramos [1,2,c], José Javier Serrano-Olmedo[1,2,d], and R. Martínez-Murillo [2,3,*]

[1]Centro de Tecnología Biomédica (CTB), Universidad Politécnica de Madrid (UPM), Campus de Montegancedo, 28223, Pozuelo de Alarcón, Madrid, Spain.

[2] Consorcio de Investigación Biomédica en Red de Bioingeniería, Biomateriales y Nanomedicina (CIBER-BBN), Spain.

[3]Neurovascular Research Group, Department of Translational Neuroscience, Instituto Cajal, CSIC, Av. Dr. Arce, 37, 28002 Madrid, Spain.

*Corresponding author: r.martinez@cajal.csic.es

Key words: CT-2A cells; hyperthermia; glioblastoma; gold nanorods; tumor progression

1.Abstract:

Metallic nanorods are promising agents for a wide range of biomedical applications. We report an optical hyperthermia method capable of inducing slowdown tumor progression of an experimental *in vivo* CT-2A glioblastoma tumor. The tumor model used in this research is based on the transplantation of mouse astrocytoma CT-2A cells in the striatum of mice by intracranial stereotaxic surgery. Two weeks after cell implant, the resulting tumor is treated by irradiating intratumoral injected gold nanorods, biofunctionalized with CD133 antibody (B-GNRs), using a continuous wave laser. Nanoparticles convert the absorbed light into localized heat due to the effect of surface plasmon resonance.[1] A significant slowdown in CT-2A tumor progression is evident, by histology and magnetic resonance imaging (MRI), at one and two weeks after irradiation treatment: 15% to 75% tumor size reduction as compared to the control untreated groups.[2] Thus, laser irradiation of B-GNRs is found effective for the treatment of CT-2A tumor progression. As the CT-2A tumor model in this research exhibits common features with the human astrocytoma disease, hyperthermic treatment by irradiating intratumoral B-GNRs might constitute a promising alternative procedure of choice to treat the progression of this deadly disease.[3]

2.Introduction

Cancer is the second leading cause of death in the world; in 2015 caused 8.8 million deaths. According to the World Health Organization [1] nearly one out of six deaths in the world is due to this disease. Primary brain tumors represent one of the most challenging forms of neoplasia to be treated. High-grade gliomas, including glioblastoma multiform (GBM) are the most aggressive type of primary brain

Summary of Comments on

Page: 2

Number: 1 Author: Reviewer Subject: Inserted Text Date: 3/12/2019 10:19:31 AM
Quantitative information is missing what are the achieved temperatures?

Number: 2 Author: Reviewer Subject: Inserted Text Date: 3/12/2019 10:18:43 AM
Please provide statistical result, p<?

Number: 3 Author: Reviewer Subject: Inserted Text Date: 3/12/2019 10:12:03 AM

tumor and despite medical intervention the median survival is only 12–15 months and 5-year survival is less than 5% GMB.[2–4] Infiltrating cancer cells beyond the boundaries of the tumor edge are responsible for tumor recurrence as well as radiation and chemotherapy resistance.[5]

In recent years nanomedicine has been progressing rapidly and it has been defined as the use of materials with dimensions in the nanometric scale range for a specific diagnostic or therapeutic purpose. These advances in nanotechnology have allowed the development of gold nanostructures with optical properties that are useful in biomedical applications, like drug delivery, hyperthermia therapy, and image contrast agents due to their biocompatibility and optical tenability.[6,7] Gold nanoparticles are highly appealing for cancer diagnostics and therapy because gold is almost an inert material (high resistance to corrosion), has low toxicity and it is easy to anchor biocompatible ligands to its surface.[8]

The gold nanoparticles used in this study are nanorods (GNRs) coated with protein G. Protein G is a common receptor for mechanically anchoring antibodies. Nanorod type has been the gold nanoparticles of choice because they are quite used in biomedical applications.[6,9,10]

Biofunctionalization of gold nanoparticles techniques are well-known procedures for biomedical technologies both *in vitro* and *in vivo*.[10,11] Applications of gold nanoparticles for hyperthermia *in vivo assay* with animals have been reported.[11–14] Experimental neurooncology demands the creation of appropriate animal models to assess the efficacy of innovate approaches for the treatment of human tumors. This is the case of CT-2A astrocytoma model.[15,16] This model is used in this study for therapeutic screening in preclinical trials. Imaging technologies in the CT-2A

Page: 3

Number: 1 Author: Reviewer Subject: Inserted Text Date: 3/12/2019 10:21:04 AM
Provide additional references, preferably recent

Number: 2 Author: Reviewer Subject: Underline Date: 3/12/2019 10:26:58 AM

Number: 3 Author: Reviewer Subject: Inserted Text Date: 3/12/2019 10:27:20 AM
this is introduction not materials and methods.

Number: 4 Author: Reviewer Subject: Underline Date: 3/12/2019 10:24:01 AM

Number: 5 Author: Reviewer Subject: Inserted Text Date: 3/12/2019 10:25:46 AM
That is not a scientific reason .
There is plenty of literature on rods vs spheres.

Provide scientific reasoning for use of rods over spheres

Number: 6 Author: Reviewer Subject: Underline Date: 3/12/2019 10:26:18 AM

Number: 7 Author: Reviewer Subject: Inserted Text Date: 3/12/2019 10:26:27 AM
formatting

Number: 8 Author: Reviewer Subject: Inserted Text Date: 3/12/2019 10:31:42 AM
Again this is introduction not materials and methods section. Provide information on available current sate-of-art animal models and their benefits or limitations

model measuring tumor growth would provide insights on B-GNRs efficacy. This cell line overexpresses the membrane receptor CD133.[14] Recently, CD133 antibodies have been employed in nanomedicine, oriented towards hepatocellular carcinoma.[17] Since the CT-2A tumor model exhibits common features with the human astrocytoma disease, it becomes an excellent candidate to assay new anticancer procedures.[18,19]

Based on using B-GNRs, together with Laser irradiation (808nm wavelength continuous wave laser source), we provide here evidence that our hyperthermia procedure provides basis for a new anti GBM therapy. This paper reports for the first time beneficious effects of this technology limiting intracranial CT-2A mouse astrocytoma tumor progression. The B-GNRs used in the present study showed high cytocompatibility, as previously reported *in vitro*.[7,17] Twenty-Seven C57BL/6 laboratory mice were stereoataxically inoculated with CT-2A glioblastoma cells, administered directly in the striatum. After two weeks of tumoral grown the resulting tumors were treated with the optical hyperthermia technique described below. To analyze the tumor volumes, measurements were performed by in vivo MRI. The data show arresting in tumor growth in treated mice as compared with their respective controls. Reduction in tumor volume was between 15 and 75%.

Glioblastoma is highly infiltrative, thus resection is problematic and recurrence frequent. The photothermal treatment would complement the resection surgery of the solid tumor mass by treating infiltrated tumor cells within tumor environment. Essays combining surgical resection of tumors and optical hyperthermia treatment, are also in course.

Page: 4

Number: 1 Author: Reviewer Subject: Inserted Text Date: 3/12/2019 10:33:05 AM

I

Number: 2 Author: Reviewer Subject: Inserted Text Date: 3/12/2019 10:37:56 AM

reads more like a results section.

Suggestion: briefly introduce the reader what except in the following sections

3.Results and Discussion:

The experiments have been performed in an orthotopic mouse model of malignant mouse astrocytoma: CT-2A, in terms of histopathological characteristics and angiogenic features.[15,16] The animal model has been produced after an intracerebral injection of CT-2A cells [20,21] into the CP. The resulting CT-2A tumor model exhibited common features with the human astrocytoma disease, as shown by histopathology, immunohistochemistry, and non-invasive imaging procedures (MRI) (Figure 1 and 2, and 4 and 6). Given that tumor-host interactions are organ specific, mouse models should be orthotopic to better reproduce their biology. It is also important to take into account on the contribution of the immune system. For this reason the animal model was accomplished in immunocompetent syngeneic mice.

3.1.Tumor growth: CT-2A cells grew in vitro as a monolayer of fusiform shaped cells. Five to ten days following intracranial injection with CT-2A cells, a soft, non-cohesive hypercellular mass was observed near the injection site (Figure 1 and 4). Three to four weeks following cell implant, a highly angiogenic and haemorrhagic soft tumor was detected (Figure 2 and 4). The tumor margins were typically well defined, merging discernibly with the adjacent white and gray matter. Histological analysis showed characteristic features of a high-grade astrocytoma, such as high mitotic index, microvascular proliferation and cellular density (Figure 1 and 4) and a central area of necrosis (Figure 6) as previously reported by our laboratory.[15] Under the electron microscope, tumor cells were pleomorphic, either large fusiform or small, with characteristic nuclei which exhibited areas of heterochromatin and frequent prominent nucleoli (Figure 3). The cytoplasm contained abundant

mitochondria and polyribosomes, indicating a high metabolic and synthetic rate. The tumors showed extensive heterogeneity.

3.2.MRI analysis: The recognition of intracranial tumors was markedly enhanced with prior administration of Gadolinium, with a resolution limit of 0.8-1 mm^3. Conventional T1- weighted (Gadolinium post-contrast) MRI provided exceptional sensitivity in detecting and delineating the location of intracranial tumors (Figure 1A,B, and 2B and 5 and 6). T1-weighted imaging with Gadolinium enhancement of vascularity was routinely used to detect tumor location, margins, size, and growth. The MRI images regarding tumor size and location correlated accurately with the results of the histopathological analysis in this study (Figure 2). T1-weighed images revealed a well-defined heterogeneously enhancing mass that arose in the CP (Figure 1A,B and 5A), extending over time rostro-caudally and eventually involving the cerebral cortex and hippocampus (Figure 2B and 6B,D**)**. Tumor progression was verified by serial MRI over time, and weekly images of experimental CT-2A tumors were successfully obtained (Figure 5 and 6**)**. The experimental tumor was characterized by rapid growth being barely detectable at 1 week post-injection and becoming unbearable at 4 weeks (Figure 2B and 5B). At that time mice began to present neurological complications and had to be sacrificed. Tumor growth resulted in marked deformation of the lateral and dorsal third ventricles. A central hypo-attenuation of the tumor was frequently seen in T1-weighted images suggesting central necrosis (Figure 5B), which was confirmed in the histological analysis of those cases. Tumor growth provoked signs of destruction of brain parenchyma and of increasing pressure within the brain as it invaded the neighboring brain structures. After 20-25 days post implantation, mice began to show signs of raised intracranial pressure. Symptoms such as lethargy or

Page: 6

Number: 1 Author: Reviewer Subject: Inserted Text Date: 3/12/2019 10:59:53 AM
what is the frequency every 2 days?

motor dysfunction with hunched posture, poor grooming, failure to thrive and weight loss, were common. The periphery of the tumor had in all instances a well-established blood supply as revealed by the enhanced pattern in T1-weighted images with Gadolinium (Figure 2B).

3.3.Immunohistochemistry: Light microscopy immunocytochemistry for CD133 and Ki67 revealed numerous positive CT-2A cells in the tumor mass (Figure 4). ki67 shows intense nuclear staining (Figure 4A,B) whereas CD133 was exclusively cytoplasmatic, with the reaction product accumulated in puncta in the cytoplasm of tumor cells (Figure 4C). Particularly, Ki67 staining accumulated in the tumor edge. Numerous Ki67 positive cells were detected within the tumor mass, being more abundant in the tumor rim and near blood vessels (Figure 4A,B). Double immunofluorescence for BrdU and nestin revealed that whereas BrdU-positive cells were abundant in the tumor mass, Nestin-positive cells also exhibiting BrdU staining were exclusively located in tumor endothelial cells (Figure 4D). The latter correlated with previous studies that Nestin is a marker for proliferative endothelium in gliomas.[22] We can therefore conclude that the CT-2A tumor model used in this research exhibited common features with the human glioglastoma disease, as shown by histopathology, immunohistochemistry, and non-invasive imaging procedures (MRI).

3.4.Electron microscopy: Under the electron microscope, subcellular immunoreaction end-product using B-GNRs antibody compound (see section 3.5) as primary antibody was carried out. Occasional B-GNRs immunolabeling bound to the nuclear membrane, whereas the majority of B-GNRs immunoreaction product is intracellular, associated with intracellular organelles (Figure 3C,D).

3.5.Efficacy of Biofunctionalization: To test the efficacy of B-GNRs as a tool to bound tumor cells, we examined by immunohistochemistry the subcellular location of B-GNRs in tissue sections after in vivo injection (see 3.3, Histopathology). Tissue sections were processed to detect endogenous CD133 using the sample resuspension of B-GNRs as primary antibody (see section 3.5). Immunohistochemistry was carried out as shown for CD133 immunohistochemistry in section 3.3 (histopathology). For this reason, resuspended B-GNRs, diluted 1:100 in PBS containing 0.2 % Triton X-100, was used as primary antibody. Tumor sections, 40-µm-thick, were incubated overnight at 4ºC with continuous stirring. Then, tissue sections were thoroughly washed and processed for immunohistochemistry following the same steps as for CD133 immunohistochemitry in section 3.4. By light microscopy, we found the reaction-end product labelling exclusively proliferating CT-2A cells, following the same cellular distribution as that observed for CD133 immunohistochemistry (Figure 3B). The latter suggesting that GNRs consistently beared anti- CD133 antibodies. Electron microscopic results were consistent with this.

3.6.Temperature measurements: in order to corroborate the generation of an adequate increase in temperature to eliminate cells by hyperthermia, changes in temperature were determined in situ, after the injection of the B-GNRs as described in section 3.8. The results show that in the control group (PBS) the temperature increase was: 40.0 ± 0.5 º C. In striking contrast, the group injected with B-GNRs and later irradiated with laser the elevation of the temperature was: 43.0 ± 1.0 º C. These values were in agreement with results by previous reports.[23]

3.7.Photothermal therapy: Tumor growth was analyzed at two time points: Week 1 (one week after laser irradiation; three weeks after cell implant) and Week 2 (two

Page: 8

Number: 1 Author: Reviewer Subject: Inserted Text Date: 3/12/2019 11:12:21 AM
for how long?

Number: 2 Author: Reviewer Subject: Inserted Text Date: 3/12/2019 11:02:24 AM
provide a Temperature vs treatment time graph

Hyperthemia dose-metric is CEM43. Report the CEM43 values

weeks after laser irradiation, four weeks after cell implant), that is 168 hours and 336 hours, respectively, after laser irradiation of endogenously administered B-GNRs (CD133-GNR, 18 animals) and control PBS+Laser (Control, 9 animals) groups. Figure 5 shows differences in tumor volume ratios between groups, CD133-GNRs and control. The graph shows the tumor evolution as a percentage of the tumor volume with respect to the total brain volume. The tumor volume was measured by MRI (Figure 6) at different post-treatment times: 'Week 1' and 'Week 2', following vehicle control (PBS+Laser) and B-GNRs + Laser (CD133-GNRs) post-treatments. At Week 1, CD133-GNRs group showed a significant reduction in tumor volume with regard to control ($p=0.03$): 1.8% vs 4.7 %, with respect to the brain size. It is noteworthy that differences in tumor progression between these group became highly significant ($p=0.008$) at Week 2: 8.1% vs 22.9 with respect to the brain size. These data support the idea that intratumoral CD133-GNRs +Laser treatment exerts a potent tumoricidal effect in the CT-2A mouse astrocytoma model.

In this study, B-GNRs+laser treated mice showed a clear behavior of tumor reduction. Tumors were analyzed in consecutive weeks 1 and 2 after hyperthermia treatment (Figure 6). Panels in Figure 6 correspond to MRI of the same brain section of a two representative mice, control (PBS+laser, Figure 6 A,B) and treated (B-GNRs+laser, Figure 6 C,D) acquired in weeks 1 (Figure 6A,C) and 2 (Figure 6B,D) after laser irradiation. The initial tumor mass in the striatum was faint one week after B-GNRs+laser irradiation (Figure 6 C) comparing to control (Figure 6 A). In the B-GNRs+laser group (Figure 6C,D) the tumor mass showed a progressive decline, from 0.68 % in 'Week1' (3 mm^3), to 0.37 % in 'Week 2' (2

Page: 9

Number: 1 Author: Reviewer Subject: Highlight Date: 3/12/2019 11:06:29 AM

Number: 2 Author: Reviewer Subject: Inserted Text Date: 3/12/2019 11:10:22 AM
short duration.

Number: 3 Author: Reviewer Subject: Sticky Note Date: 3/12/2019 11:08:33 AM
Material and Methods section says 3 groups control, PBS+Laser, B-GNR+ Laser.

Here only two groups are reported.

What about B-GNR without Laser?

Number: 4 Author: Reviewer Subject: Inserted Text Date: 3/12/2019 11:16:48 AM
How may animals survived past week 2.
Are there any tumor size results from the animal fro Week 3 & 4 after AT (diagram 1)

mm^3) and 0.22 % in 'Week 3' (0.99 mm^3), comparing the total brain size, reaching a minimum value of 0.17%, four weeks after treatment (Figure 6D) .

4Conclusions

This study shows the efficacy of B-GNRs +Laser treatment promoting the tumoricidal effect of the optical hyperthermia on an in-vivo CT-2A astrocytoma model. This treatment constitutes a promising alternative choice to treat intracranial neoplasms in humans. Reduction of intracranial tumor volume following this procedure can be considered as an outstanding achievement in the treatment of this deadly cancer that opens new avenues in the comprehension and treatment of primary brain cancer, supporting future research in this field.

5Materials and methods

5.1.Cell culture: CT-2A mouse astrocytoma cells were obtained as a generous gift from Prof. T.N. Seyfried (Boston, MA, USA). Tumor cells were grown in RPMI 1640 medium (Gibco, Invitrogen Co., Carlsbad, CA, USA) supplemented with 10% heat-inactivated fetal bovine serum (R10) in a humidified atmosphere containing 95% air and 5% CO_2 at 37 °C. Upon reaching confluency, the cells were trypsinized and collected. The pellet was resuspended in RPMI 1640 medium and the cell suspension was adjusted to obtain an appropriate concentration of cells for injection (8×10^4 cells in 4 µL).[24]

5.2.Mouse tumor model: A total of three experiments were conducted using four-month old C57BL/6 mice (35.26 g ± 1.01 body weight). Each experiment consisted in 3 controls, (PBS+laser treated animals) and 6 treated (B-GNRs+laser). The animals were housed with free access to food and water in an animal room with a controlled temperature and a natural light cycle. Daily routines were performed

Page: 10

Number: 1 Author: Reviewer Subject: Sticky Note Date: 3/12/2019 11:04:25 AM
this sentence is confusing

Number: 2 Author: Reviewer Subject: Highlight Date: 3/12/2019 11:03:56 AM

Number: 3 Author: Reviewer Subject: Inserted Text Date: 3/12/2019 10:38:49 AM
why four month old?

Number: 4 Author: Reviewer Subject: Inserted Text Date: 3/12/2019 10:39:42 AM
B-GNR without laser group is missing

between 7 a.m. and 4 p.m. by authorized personnel. CT-2A cells were injected into the right caudateputamen (CP) of twenty-seven experimental animals by intracranial injection using stereotaxic guidance. Mice were deeply anesthetized with inhaled isoflurane (Isoflo) and placed in a mouse stereotaxic frame (David Kopf Instruments, Tujunga, CA, USA). While under deep anesthesia, a sagittal incision was made through the skin to expose the skull, and a burr hole was drilled at 0.1 mm anterior and 2.25 mm lateral to bregma. A 10 μL Hamilton syringe (Hamilton, Reno, NV, USA) with a 27-gauge needle was inserted from brain surface at 4 mm depth for infusion of tumor cells. The tumor cells were injected in a volume of 0.15 μL for a time frame of 15 min, this amount was equivalent to approximately 3000 cells. Two weeks after cell implant, adequate cell proliferation was confirmed by MRI, H&E staining and immunohistochemistry and (Figure 1 and 2 and 4). Two weeks after tumor cell implantation, the presence and size of generated brain tumor was evaluated by MRI (Diagram 1). All procedures were performed under the Spanish Regulations for animal experimentation (Laws 53/2013 and ECC/566/2015) on animal experiments and with the Ethical Committee of the Spanish Council for Scientific Research (CSIC). All these experiments and measurements were made using a thermal blanket to keep the temperature of the body mouse stable and thus prevent the temperature from falling due to anesthesia.

5.3.Histopathology: All mice were clinically evaluated and sacrificed at different time intervals, 14, 21, and 28 days following cell implants. Experimental animals were sacrificed when they showed signs of motor dysfunction or exhibited symptoms consistent with failure to thrive as per animal care protocols. Histopathology was performed on coronal tissue sections obtained through the same rostro-caudal levels

Page: 11

Number: 1 Author: Reviewer Subject: Underline Date: 3/12/2019 10:41:32 AM

Number: 2 Author: Reviewer Subject: Underline Date: 3/12/2019 10:41:37 AM

Number: 3 Author: Reviewer Subject: Inserted Text Date: 3/12/2019 10:42:08 AM

Be consistent and use Figure only

that were previously identified by MRI (Figure 1) as exhibiting tumor growth. Mice were deeply anesthetized as for MRI and then perfused transcardially through a blunt cannula with 20 mL Phosphate-Buffered Saline from Gibco (PBS) followed by 40 mL of 4% paraformaldehyde in 0.1 M phosphate buffer (PB), pH 7,4. Brains were then removed and post-fixed for 4 hours by immersion in the same fixative, at room temperature. For H&E stain tissue blocks were paraffin embedded and then cut coronally in 5-µm sections (Figure 1B,C). For light microscopy immunohistochemistry, brain tissue was sectioned at 40-µm-thick in the coronal plane with the aid of a vibratome (Leica Microsystems GmbH, Wetzlar, Germany).

5.4.Immunohistochemistry: The expression of the CD133 protein in the experimental tumor was evaluated using polyclonal antibodies (Sr John´s laboratories, STJ201168). Ki67 immunostaining using polyclonal antibodies (ab15580 abecam) was also carried out to evaluate cell proliferation.[25] Immunohistochemistry was performed according to standard avidin-biotin-peroxidase complex (ABC) methods.[26] Immunohistochemistry for CD133 and Ki67 was carried out in free-floating sections that were preincubated in 1% H_2O_2 in PBS for one hour to block endogenous peroxidase. Sections were then treated with 3% normal serum obtained from the species providing the secondary antibodies diluted in PBS containing 0.2% Triton X-100, for 1 h at room temperature (RT). Then, sections were incubated overnight at 4ºC in the primary antibodies diluted in PBS containing 0.2% Triton X-100. Antibodies dilutions were: i) CD133, 1:500 and ii) Ki67. After washing thoroughly in PBS, histological sections were incubated with biotinylated secondary antibodies, goat anti-rabbit immunoglobulins 1:200 in PBS (Vector Laboratories, Burlingame, CA, USA) for 1 h at RT. After additional washes, sections were incubated with peroxidase-linked ABC (Vector Laboratories) for 90

Page: 12

Number: 1 Author: Reviewer Subject: Inserted Text Date: 3/12/2019 10:42:51 AM
Reference for published or standardized procedure

min. Peroxidase activity was developed by nickel enhanced 3,3'-diaminobenzidine tetrahydrochloride (DAB) as described.[27] Finally, sections were washed, mounted and dehydrated for light microscopy visualization. Histological sections were examined with a Zeiss Axiophot II microscope (Zeiss Iberica, Madrid, Spain) and images captured with a digital camera (DMC le, Polaroid, Cambridge, MA, USA). The method of BrdU labeling was also used for in-vivo tumor cellular proliferation studies, following a procedure previously published by the laboratory.[28] As nestin was found as a marker for proliferative endothelium in gliomas,[22] we combined its immunocytochemical expression with BdrU immunostainig in our tumor model by immunofluorescence. Immunofluorescence staining for confocal microscopy was carried out by incubating tissue sections in the specific rat antibody for BrdU (1:2000, abcam) and rabbit antibodies for nestin (1:000, Sigma-Aldrich, SAB4200347). Sections were then thoroughly washed with PBS, primary antibodies were visualized using the corresponding Alexa-conjugated secondary antibodies, e.g. Alexa Fluor® 488 donkey anti-rabbit, and Alexa Fluor® 568 goat anti-rat (1:1000, Invitrogen, Molecular Probes) for 2 h at RT and mounted on glass slides with anti-photobleaching mounting media (DABCO/Mowiol). For control experiments, slices were stained with secondary antibodies only. Sections were counterstained with 4,6-diamidino-2-phenylindole (DAPI, 300 nM in PBS, Invitrogen) and examined on a LEICA TCS SP5 scanner confocal microscope (Leica Microsystems GmbH, Wetzlar, Germany). For control experiments, slices were stained with secondary antibodies only.Cy3-donkey anti-mouse IgG and Rhodamine Red donkey anti-rabbit IgG (Jackson ImmunoResearch, West Grove PA, USA) diluted 1:200 in PBS, for 1 hour at RT. Confocal images were acquired using a Leica TCS SP5 (Leica Microsystems GmbH, Wetzlar, Germany) scanner.

No immunolabeling was detected when the primary antibodies were omitted or replaced with an equivalent concentration of normal mouse or rabbit serum. In addition, preabsortion with an excess of the antigen prevented staining in all cases.

5.5.Biofunctionalization of gold nanoparticles with CD133 antibody: Protein G captures a wide range of Ig's, including rabbit IgG, via the IgG Fc-region. Thus, GNRs were coupled to protein G compound for biofunctionalization with CD133 antibodies. GNRs (10×40nm C12-10-808-TPG-50, NANoPARTz, OD/ml: 50) were tuned to the laser source, with a surface plasmon resonance peak (longitudinal band) at 808 nm, commercial GNRs-protein G were resuspended thoroughly in PBS to obtain a homogeneous suspension. For the Ig capture, 100µl of GNRs-protein G solution was transferred to a tube at RT and washed in PBS several times by centrifugation 5 minutes at 14.5 rpm, at RT. Then, polyclonal antibodies against CD133 (St John´s laboratory, STJ 20168) were added at a 1:500 final dilution in a solution made of 100 µL of washed nanoparticles-protein G in 500 µL 3% BSA. The mixture was incubated for 1 hour with gentle rotative agitation, at 4ºC. The mixture was then washed three times in 600µL 3% BSA by centrifugation 5 minutes at 14.5x1000 rpm, at RT. After the last centrifugation, B-GNRs (GNRs-protein G-CD133 compound) were resuspended in 100µl PBS.

5.6.Optical Hyperthermia Device: A continuous laser wave (MDL H808, PSU-H-LED power source; Changchung New Industries, Changchun Jilin, China) working at 808 nm, with a maximum output power of 5 W, a beam height from base of 29 mm, a beam diameter with an aperture of 5–8 mm^3, and a laser head dimensions of 155×77×60 mm^3 was used in this study. The laser was connected to the system via a multimode optical fiber with a core diameter of 600 µm, a length of 1.5 m, and a power transmission of 90–99% (600 µm MM fiber; Changchung New Industries).

The optical fiber was fixed to the stereotaxic device, suspended vertically through a collimation lens (78382, Newport, Irvine, CA) with the downward facing at power density of 3.55 watts/$cm^{2,}$ using a Newport power meter model 843-R with a Newport 818-SL photodetector.

5.7.Photothermal therapy: Two weeks after of tumor cell implantation, mice were weighed, and then anesthetized with 1% isofluorane. Randomly selected animals were processed for photothermal therapy. Using the same surgery protocol as in section 3.2 (Mouse tumor model**)**, 2μL of B-GNRs were injected at 4 mm depth, the same place where the tumor cells were previously injected two weeks before, at a rate of 0.5μL/min. After 5 minutes, a second dosage of 2μL was then injected at 2 mm depth by raising the needle appropriately. 10 minutes following the second injection, the needle was withdrawn. In summary, a total of 4 μL of B-GNRs were injected. The laser was focused through the same burr hole previously used to inject the tumor cells and the B-GNRs. The radiation process was carried out for 25 continuous minutes. The procedure was replicated for three consecutive days to eighteen mice called a treated group, six mice per group (Diagram 1).

5.8.Temperature measurements: A thermal probe (Luxtron Corporation) was introduced into the brain tissue through an additional 1mm burr hole (Diagram 2) in order to analyze the magnitude of the temperature increase following laser irradiation of the B-GNRs particles detected as described in section 3.7. The experiment was carried out in three animals subjected to the same nanoparticle injection protocol and illuminated with a laser for 25 minutes. Samples were recorded every second using the software supplied by the manufacturer in software LabView 2011.

5.9.MRI acquisition: MRI was performed at the Nuclear Magnetic Resonance (NMR) and Electronic Spin Center of the Universidad Complutence de Madrid (UCM) using 1 Tesla benchtop MRI scanner [Icon (1T-MRI); Bruker BioSpin GmbH, Ettlingen, Germany]. The system consists of a 1 T permanent magnet (without extra cooling required for the magnet) with a gradient coil that provides a gradient strength of 450 mT/m. The animal monitoring systems and the solenoid mouse head RF coil for the 1T-MRI were integrated into the bed and they allowed the animals to be handled on with accurate positioning of the coil and full control of anesthesia and body temperature. Fifteen minutes before placing the mouse into the MRI bed, mice were injected intraperitoneally with 0.4 mmol/Kg Gadopentetate dimeglumine (Gadolinium, Magnevist, Schering, Germany). Animals were anaesthetized with a mix of isofluorane in oxygen (2% for induction and 1% for maintenance). In order to evaluate the tumor volume MRI experiment consisted of two dimensional pre- and post-contrast Fast Spin Echo (FSE) T1 and T2 weighted images (T1WI, T2WI). Both sequences were acquired with the same geometry and resolution: field of view of 20 × 20 mm, number of slices of 15, slice thickness of 1 mm, matrix size was 160 x 160 that was reconstructed to 200 x 200, final resolution of 0.100 x 0.100 mm. T2WI parameters were as follows: repetition time/echo time (TR/TE), 3040/96 ms; 12 averages, echo train length, 12; acquisition time ~ 8 minutes. T1WI parameters were: TR/TE, 262/6 ms; 36 averages, echo train length, 2; acquisition time ~ 12 minutes. Measurements were performed three and four weeks post CT-2A inoculation. The tumor volume was analyzed using the free software ImageJ 1.50i. In all cases, both absolute and relative tumor volumes, normalized with respect to the total brain volume were measured. The images were repeated one week later for all individuals. In cases showing a clear survival trend,

two weekly additional MRI studies were carried out, up to a total of four scans (see Diagram 1).

5.10. Ultrastructural studies: The experimental tumor treated with gold nanoparticles CT-2A activated with CD133 was cut, in 40-µm-thick tissue sections, using a vibratome. For the subcellular location of gold nanoparticles, tissue sections were processed as for light microscopy, except that Triton X-100 was avoided in the incubation steps. The sections were washed for 5 min in PBS first and then in 0,1M PB, postfixed in 1% osmium tetroxide in 0.1M PB for 1 hour, dehydrated in ethanol of increasing concentrations and block-stained in uranyl acetate (1% in 70% ethanol) in the dark for 40 min at room temperature. The sections were then flat embedded and mounted on Durcupan ACM resin slides (Sigma-Aldrich Inc.) under plastic coverslips and cured for 3 days at 56°C. Selected areas of the tumor were dissected out and re-embedded in Durcupan. Ultrathin sections were obtained with the aid of a Reichert OM U3 ultramicrotome (Reichert, Germany), mounted on formwar-coated grids, stained with lead citrate, and examined under a Jeol 1200 electron microscope (Jeol, Tokyo, Japan) at 80 Kv.

5.11. Statistical analysis: Statistical Package for the Social Sciences (SSPS) software was used for all statistical tests. All values are expressed as mean ± the standard error of the mean (S.E.M.). When applicable, statistical significance was assessed by Student t-test for independent samples. Statistical level of significance was defined as $p < 0.05$.

6 Acknowledgements

The authors would like to thank Ms Soledad Martinez (cell culture experiments), Centre for Biomedical Technology (CTB) for technical help. Also, Ph.D Teresa López de Mora for critical reading of the manuscript. The authors are thankful to their grant supporters,

Page: 17

Number: 1 Author: Reviewer Subject: Inserted Text Date: 3/12/2019 10:50:32 AM
Not appropriate for n<20.

Review
https://www.ncbi.nlm.nih.gov/pubmed/25901488

Number: 2 Author: Reviewer Subject: Inserted Text Date: 3/12/2019 10:51:06 AM
Why t-test?

Universidad Nacional Experimental del Táchira (UNET) – Venezuela to Oscar Casanova-Carvajal. This study was also financially supported in part by CIBER-BBN (Spain). Characterization of the MNPs has been performed by the ICTS "NANBIOSIS", Unit 15 (Functional Characterization of Magnetic Nanoparticles) of the CIBER in Bioengineering, Biomaterials & Nanomedicine (CIBER-BBN) at the Center for Biomedical Technology (CTB) of the "Universidad Politécnica de Madrid" (UPM).

7References

[1] World Healh Organization, "Cancer," can be found under http://www.who.int/mediacentre/factsheets/fs297/en/, **2017**.

[2] C. L. Gladson, R. A. Prayson, W. M. Liu, *Annu. Rev. Pathol. Mech. Dis.* **2010**, *5*, 33.

[3] P. Y. Wen, S. Kesari, *N. Engl. J. Med.* **2008**, *359*, 492.

[4] R. Method, *Cancer* **1969**, *62*, 2152.

[5] T. Demuth, M. E. Berens, *J. Neurooncol.* **2004**, *70*, 217.

[6] M. Ramos, Sanchez, Martinez, Pozo, Serrano, M. Ramos, *Int. J. Nanomedicine* **2012**, 1511.

[7] X. Huang, P. K. Jain, I. H. El-Sayed, M. A. El-Sayed, *Lasers Med. Sci.* **2008**, *23*, 217.

[8] A. R. Makkouk, S. J. Madsen, in *Opt. Methods Instrum. Brain Imaging Ther.* (Ed: S. J. Madsen), Springer New York, New York, NY, **2013**, pp. 235–251.

[9] S. Avvakumova, M. Colombo, P. Tortora, D. Prosperi, *Trends Biotechnol.* **2014**, *32*, 11.

[10] T. Fernández-Cabada, C. S.-L. de Pablo, L. Pisarchyk, J. J. Serrano-Olmedo, M. Ramos-Gómez, *J. Nanosci. Nanotechnol.* **2016**, *16*, 7689.

[11] C. Yao, L. Zhang, J. Wang, Y. He, J. Xin, S. Wang, H. Xu, Z. Zhang, *J. Nanomater.* **2016**, *2016*, 1.

[12] F. Pourgholi, M. Hajivalili, J. Farhad, H. S. Kafil, M. Yousefi, *Biomed. Pharmacother.* **2016**, *77*, 98.

[13] E. S. Day, P. A. Thompson, L. Zhang, N. A. Lewinski, N. Ahmed, R. A. Drezek, S. M. Blaney, J. L. West, *J. Neurooncol.* **2011**, *104*, 55.

[14] A. Espinosa, R. Di Corato, J. Kolosnjaj-Tabi, P. Flaud, T. Pellegrino, C. Wilhelm, *ACS Nano* **2016**, *10*, 2436.

[15] R. Martínez-Murillo, A. Martínez, *Histol Histopathol* **2007**, *22*, 1309.

[16] E. Binello, Z. A. Qadeer, H. P. Kothari, L. Emdad, I. M. Germano, *J. Cancer* **2012**, *3*, 166.

[17] J. X. Jiang, H. W. Chen, C. Yu, Y. Y. Zhang, M. Y. Chen, S. Tian, C. Y. Sun, *Nanomedicine* **2015**, *10*, 1863.

[18] E. Piktel, K. Niemirowicz, M. Watek, T. Wollny, P. Deptuła, R. Bucki, *J. Nanobiotechnology* **2016**, *14*, 1.

[19] N. S. Abadeer, C. J. Murphy, *J. Phys. Chem. C* **2016**, *120*, 4691.

[20] H. M. Zimmerman, H. Arnold, *Am. J. Pathol.* **1943**, *19*, 939.

[21] T. N. Seyfried, M. El-Abbadi, M. L. Roy, *Mol. Chem. Neuropathol.* **1992**, *17*, 147.

[22] K. I. Sugawara, H. Kurihara, M. Negishi, N. Saito, Y. Nakazato, T. Sasaki, T. Takeuchi, *Lab. Investig.* **2002**, *82*, 345.

[23] R. Le Fèvre, M. Durand-Dubief, I. Chebbi, C. Mandawala, F. Lagroix, J. P. Valet, A. Idbaih, C. Adam, J. Y. Delattre, C. Schmitt, et al., *Theranostics* **2017**, *7*, 4618.

[24] L. E. Abate, P. Mukherjee, T. N. Seyfried, *J. Neurochem.* **2006**, *98*, 1973.

[25] Gang Lu Sen Mun Wai W.S. Poon D.T. Yew, *Microsc. Res. Tech.* **2005**, *68*, 255.

[26] S. M. Hsu, L. Raine, H. Fanger, *Am. J. Clin. Pathol.* **1981**, *75*, 816.

[27] S. M. J. Rodrigo, D. R. Springall, O. Uttenthal, M. L. Bentura, F. Abadia-Molina, V. Riveros-Moreno, R. Martínez-Murillo, J. M. Polak, *Philos. Trans. R. Soc. London. Ser. B Biol. Sci.* **1994**, *345*, 175 LP.

[28] V. C. Muñetón-Gómez, E. Doncel-Pérez, A. P. Fernandez, J. Serrano, A. Pozo-Rodrigálvarez, L. Vellosillo-Huerta, J. S. Taylor, G. P. Cardona-Gómez, M. Nieto-Sampedro, R. Martínez-Murillo, *Front. Cell. Neurosci.* **2012**, *6*, 1.

FIGURE LEGENDS

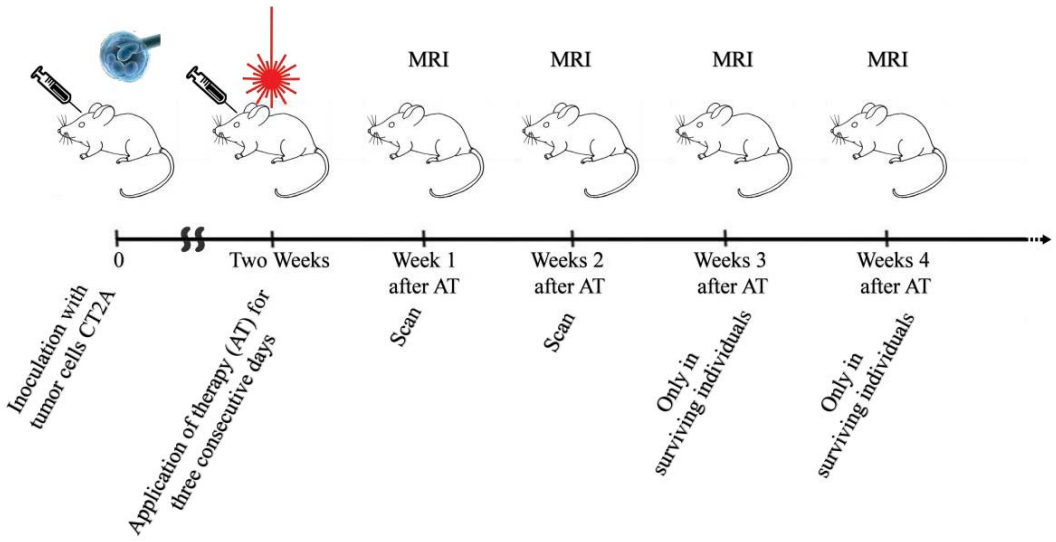

Diagram 1. Summary graph of the methodology.

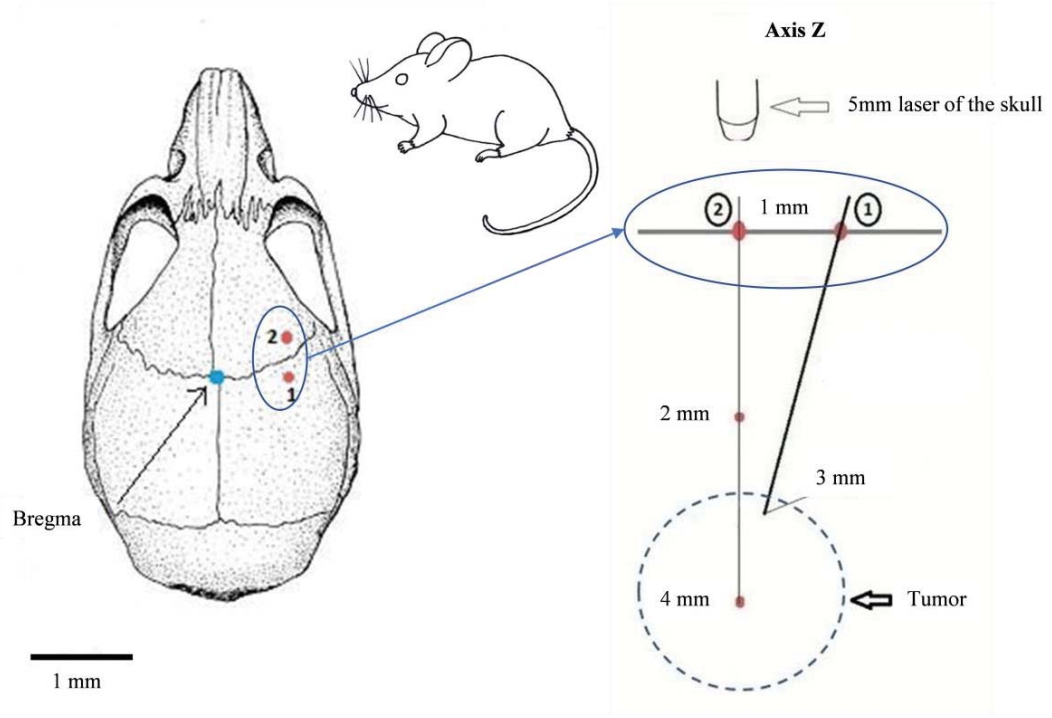

Diagram 2. Methodology of hyperthermic temperature measurements.

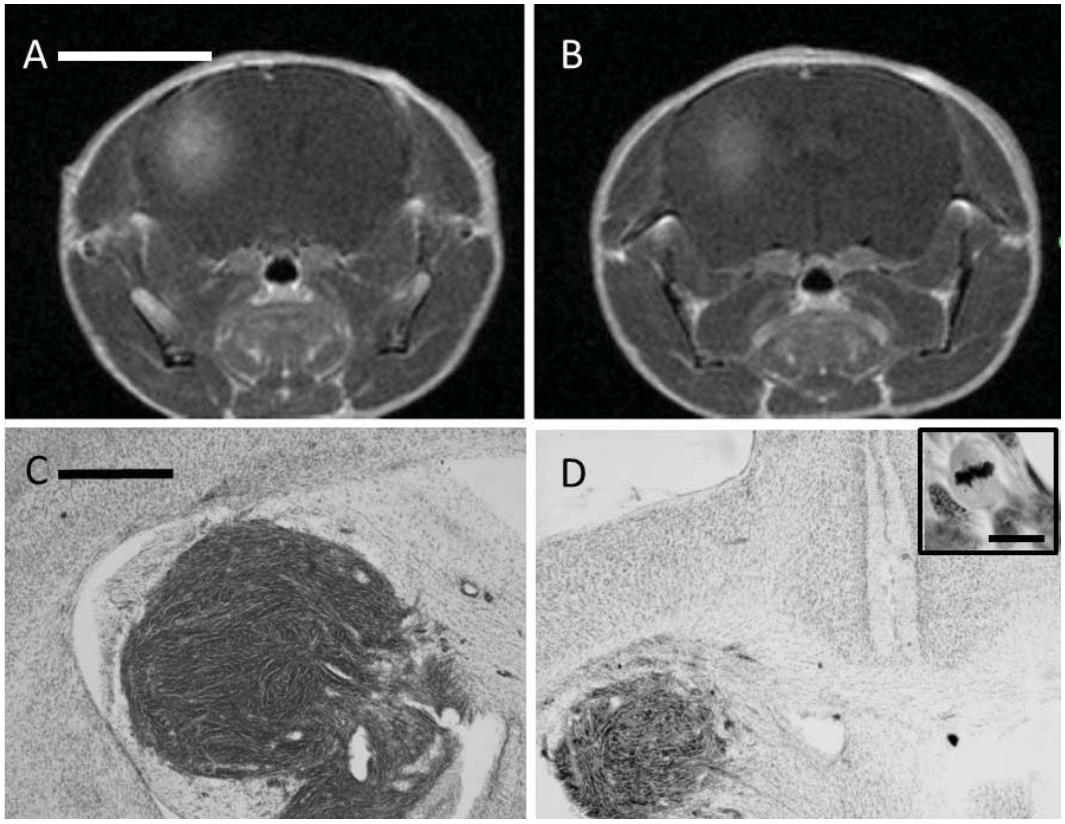

Figure 1. Cell proliferation as seen by MRI and H&E staining. Panels A, B, represent T1–weighted (Gadolinium postcontrast) images corresponding to the same experimental CT-2A tumor depicted in C, D, respectively, showing the tumor progression at different rostro-caudal levels, two weeks following cell implant. Notice that in A and B the hyperintense signal is restricted to the CP in the right hemisphere. Inset in D shows a mitotic image nearby a neoformed blood vessel. Scale bars: A,B= 5mm; C,D=1mm, inset in D=15μm.

Page: 21

Number: 1 Author: Reviewer Subject: Inserted Text Date: 3/12/2019 11:18:40 AM
indicate the region of interests with an arrow

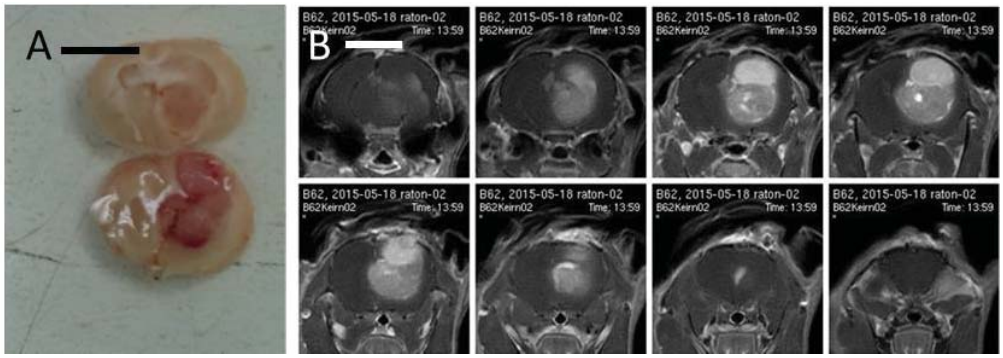

Figure 2. Characterization of CT-2A induced brain tumors. A. Coronal 1mm-thick coronal sections through the same mouse brain with a hemorrhagic CT-2A tumor mass lying in the right cerebral hemisphere, 28 days following CT-2A cell injection. The photograph was taken after in vivo MRI (B) and removal of the brain at the time of necropsy for histology. B, panels represent T1–weighted (Gadolinium postcontrast) images at different rostro-caudal levels corresponding to the same experimental CT-2A tumor depicted in A, showing the tumor progression four weeks following cell implant. Notice in B hyperintense signal in the rim of the tumor indicating that the tumor border is well-vascularized and also hypo-attenuation in central regions of the tumour suggesting necrosis. Scale bars: A,B= 4mm.

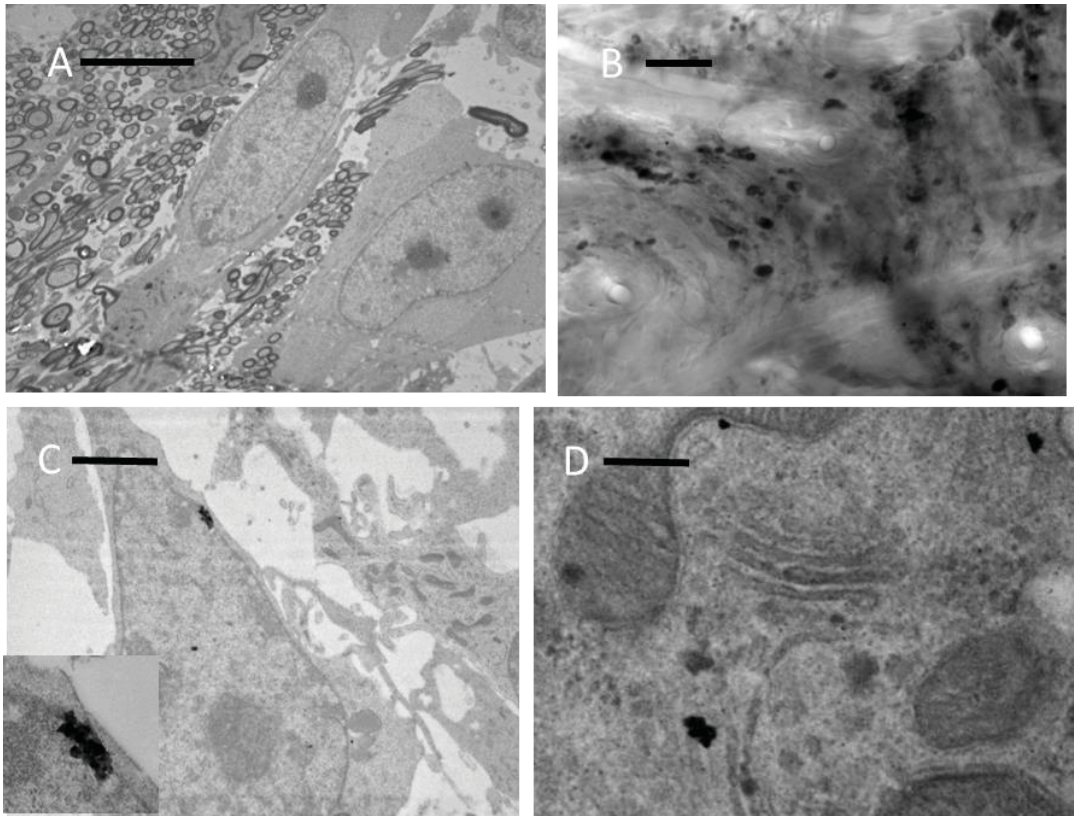

Figure 3. A. Electron micoscopic image of osmium-stained CT-2A tumor cells illustrating the ultrastructural appearance of tumor cells in the transition zone with the striatum. Tumor cells show cytological pleomorphism with prominent nucleoli, slender processes and characteristic heterochromatin. Notice adjacent myelinic fibres of the striatum in the surrounding neuropil and apparent edema, suggesting inflammation of the tissue. B, Light micrograph showing intratumoral B-GNRs deposition attached to tumor cells as revealed by immunohistochemical staining, maily nearby cappilaries. In C and D the immunoreaction product appears to label nanoparticles which accumulate intracellularly (big arrows). C and D, illustrate the subcellular location of the B-GNRs immunoreaction end-product forming complexes attached to the nuclear membrane (C) and intracellular organelles (D). E, is a higher power magnification of the reaction product shown in C showing B-GNRs immunoreactivity associated with the nuclear membrane. Scale bars: A=15μm; B=100 μm ; C=5μm; D=0,25μm.

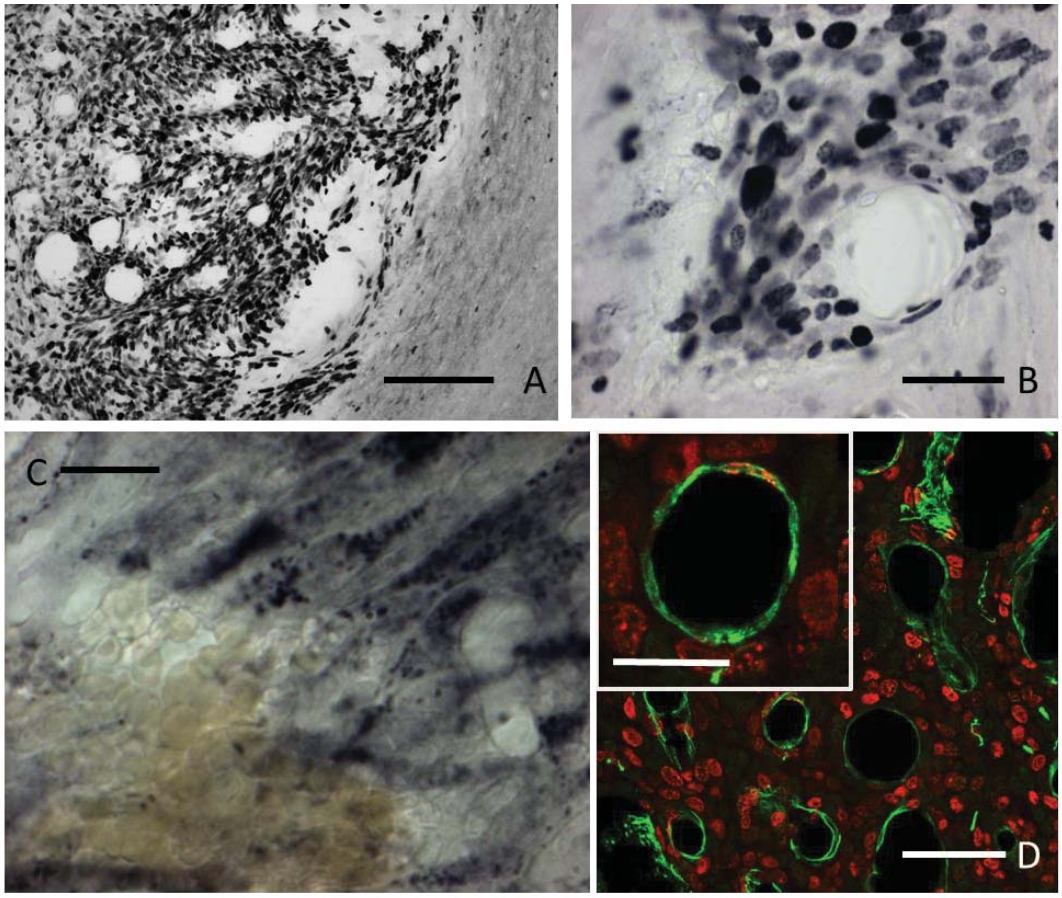

Figure 4. Immunocytochemical characterization of induced brain tumors in C57BL/6 mice, 21 days following CT-2A cell line implantation. Light micrographs A-C, illustrate Ki67 (A,B) and CD133 (C) positive cells in the tumor mass. Notice in A that numerous intratumoral blood vessels (asterisks) are seen in the tumor mass. Also in B that ki67-positive cells exhibit immunoreaction product in the cell nucleus of cells that characteristically arranged around a capillary. In addition, see in C puncta of CD133-immunoreaction product restricted to tumor cells. The yellow color at the bottom of the left hand side in C represents a hemorrhagic region. D, illustrates tumor-associated neo-angiogenesis by double immunofluorescence staining for BrdU (cell nucleus, red) and Nestin (prolifetarive endothelium, green). As previously reported for human gliomas, Nestin-immunoreactivity was found as a marker in this study for proliferative endothelium in the CT-2A model. Inset in D, shows details of an anomalous proliferating capillary. Scaler bars: A=500 μm; B=200 μm ; C=50μm; D=100μm; Inset in D=50μm.

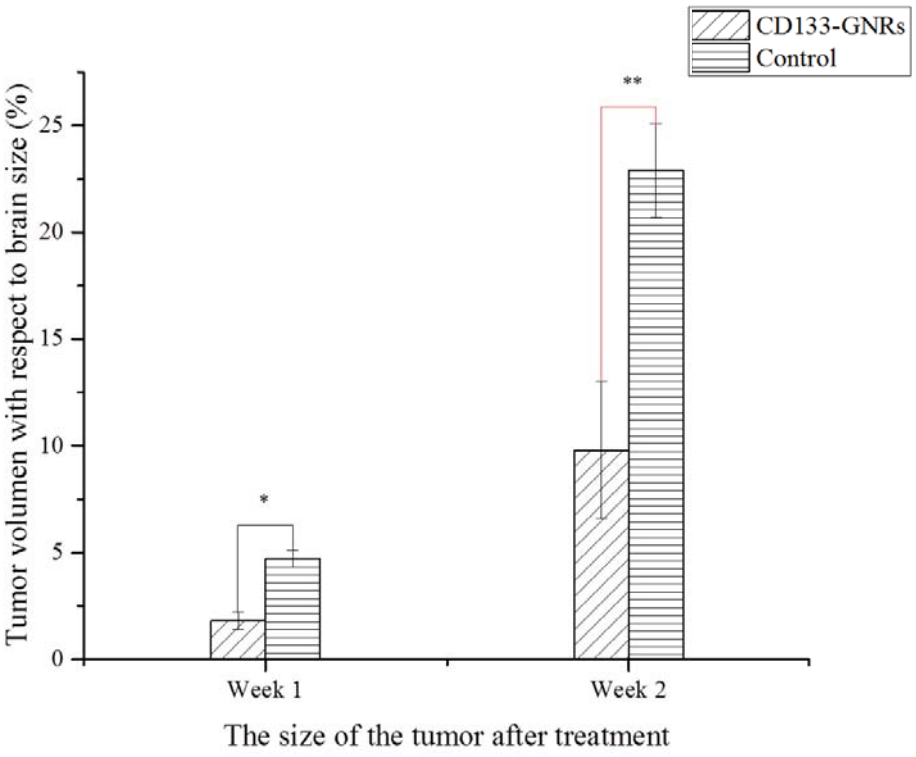

Figure 5. Tumor volume, expressed as a percentage of total brain volume, in control mice (PBS+Laser) and B-GNRs +Laser (CD133-GNRs), at Week 1 and Week 2 (time periods after laser irradiation). The data represent the mean ± SEM of n=3 independent experiments. Student-t test revealed a significant difference (p=0.03) between Control and CD133-GNRs at Week 1. The CD133-GNRs group reached higher significance benefit** at Week 2 (p=0.008).

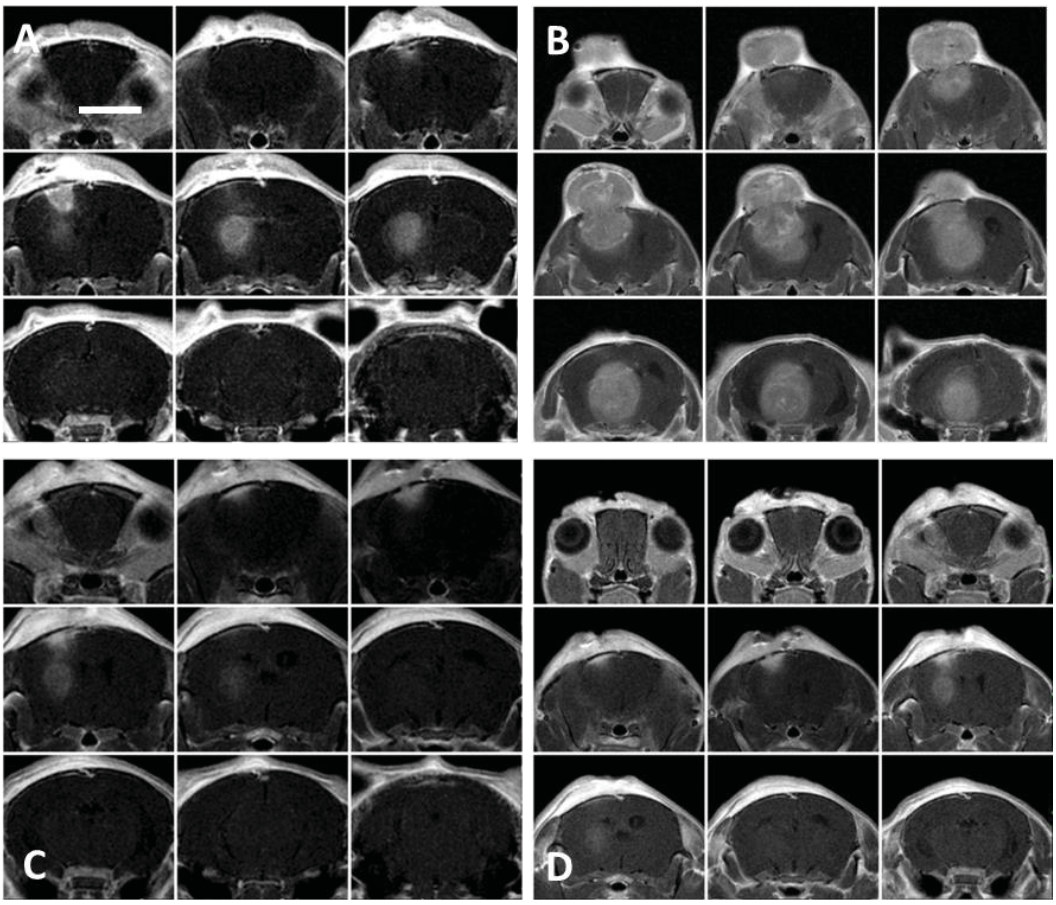

Figure 6: Shows MRI images of two mice randomly chosen from both groups: Control (A,B) and CD133-GNRs for 'Week 1' (A,C: three weeks after CT-2A implant) and 'Week 2' (B,D: four weeks after CT-2A implant) post-treatments, respectively. These images show an apparent deceleration in tumor progression in the CD133-GNRs group.